Aerosol Science and Technology, 39:519–526, 2005

ISSN: 0278-6826 print / 1521-7388 online
DOI: 10.1080/027868291004652

A Fast Scanning Mobility Particle Spectrometer for Monitoring Transient Particle Size Distributions

Sandip D. Shah and David R. Cocker III
Department of Chemical and Environmental Engineering; Center for Environmental Research and Technology, Bourns College of Engineering, University of California, Riverside, CA, USA

The Scanning Mobility Particle Spectrometer (SMPS) is a key tool for measuring particle size distribution. The application of the instrument to obtain size distributions throughout a wide range of particle sizes for transient systems, such as motor vehicle emissions, has been limited by the time resolution of the SMPS. In this paper, we present a fast-SMPS (f-SMPS) that utilizes a Radial Differential Mobility Analyzer (rDMA) and a Mixing Condensation Particle Counter (mCPC). The combination of these two components allows for the acquisition of particle size distributions on the time scale of several seconds. The instrument has an operating range of 5–98 nm and can obtain particle size distributions at rates of up to 0.4 Hz. This paper presents the initial construction and calibration of the instrument followed by its application to several sampling scenarios. Samples from the on-road testing of a heavy-duty diesel (HDD) vehicle demonstrate the utility of this instrument for motor vehicle emissions measurements as size distributions can now be associated with discrete events taking place during vehicle on-road operation. For instance, these data indicate the presence of a number peak at 15 nm during transient vehicle operation. Previous work indicates that these particles are associated with the loss of engine lubricating oil.

INTRODUCTION

Over the past 30 years, the Differential Mobility Analyzer (DMA) has been a critical tool for elucidating particulate matter (PM) size distributions. From its introduction by Knutson in 1976 to modifications made by numerous researchers, the instrument has been reliably used to measure PM size distributions in many different applications (Flagan 1998). These instruments are primarily suited for obtaining size distributions from an aerosol whose size distribution is slowly evolving, although advances such as the Scanning Mobility Particle Spectrometer (SMPS) (Wang and Flagan 1989) have provided the ability to monitor size distributions on the time scale of minutes.

Received 28 October 2004; accepted 4 May 2005.
Address correspondence to David R. Cocker III, Bourns College of Engineering, Center for Environmental Research and Technology, University of California, Riverside, CA 92521, USA. E-mail: dcocker@engr.ucr.edu

The application of the current SMPS to vehicular emissions has been limited due to its slow scanning speeds relative to the transient nature of aerosols produced during nonsteady state vehicle operation. Tests of vehicles run at steady state in chassis dynamometer laboratories, at roadside monitoring stations and in chase vehicles have been performed by a number of researchers. (Allen et al. 2001; Shi et al. 1999; Kittelson et al. 2001). However, there is a critical need for a faster version of the SMPS that is capable of dynamically monitoring transient PM size distributions resulting from rapid variations in engine operating conditions during on-road operation.

The residence time in the classifier and ability of the detector to quickly grow and count PM have limited the time resolution of the currently used SMPS. The SMPS systems currently being used at CE-CERT consists of a TSI Model 3081L cylindrical Differential Mobility Analyzer (cDMA) and a TSI Model 3760A Condensation Particle Counter (CPC) (TSI, St. Paul, MN). In its current configuration, this SMPS system can obtain size distributions at speeds on the order of 300 seconds without measurable loss of resolution due to smearing of the instrument transfer function (Collins et al. 2004). Scan speeds as fast as 30–45 seconds are attainable with the current system with consequent losses in accuracy and resolution.

Several instruments with a time resolution on the order of seconds or fractions of a second are currently available. (Caldow 2004; Keskinen et al. 1992; Moisio and Niemela 2002; Kittelson 2002; Tammet 1998; Han 2000). These instruments classify particulate matter based on electrical mobility or aerodynamic diameter and detect particles as electrical current through either a single or an array of electrometers. The use of electrometers as detectors allows these instruments to simultaneously monitor multiple channels and obtain fast size distributions. In contrast to the SMPS, the electrometer-based detection of aerosols allows instruments to constantly monitor size bins rather than scanning across a range. Although capable of obtaining fast size distributions and monitoring several channels simultaneously, these instruments have lower resolution than the SMPS due to the finite number of electrometers incorporated into those instruments.

The two differing methods of particle detection (electrometer- and CPC-based measurements) each have limitations

to their performance. In electrometer-based measurements, the lower detection limit for particle concentration is dictated by the minimum level of electrical noise (within individual electrometers and that due to neighboring electrometers) relative to the current generated by charged particles. On the other hand, CPCs count individual particles and have a lower detection limit of zero particles. The minimum detectable particle size in electrometer-based measurements is limited by the classifier utilized (Tammet 1998). The minimum detectable particle size in CPCs is limited by the ability of the CPC to grow particles to a size sufficient to be detected by a laser counter. Recently, correlations between these instruments and the SMPS have been attempted and several have been reported in the literature (Maricq et al. 2000; Khlystov 2001).

This paper describes the application of a fast-SMPS (f-SMPS) to measure transient particle size distributions of vehicular exhaust. In this work the instrument has been primarily used to measure particle size distributions from vehicular exhaust. It can also be utilized in other applications requiring the monitoring of ultrafine particle size distributions such as aircraft-based atmospheric measurements or process control in nanoparticle synthesis. The instrument consists of two major components: a radial DMA (rDMA) and a mixing CPC (mCPC). As both components have been described previously (Zhang et al. 1995; Wang et al. 2002), only a brief description will be given in this text. The advantages of these components over the commonly used cDMA and CPC are: (1) minimization of the diffusional broadening of the transfer function within the rDMA due to shorter residence time (Zhang et al. 1995); (2) better resolution of the rDMA compared with the TSI 3081L long column cDMA for PM in the range of 3–200 nm (Zhang et al. 1995); (3) high butanol reservoir operating temperatures to improve supersaturation ratios inside the CPC condenser yielding fast particle growth and the detection of particles down to a diameter of 5 nm (Wang et al. 2002); (4) turbulent mixing of the butanol and particle flows that improves mixture homogeneity, allowing for shorter particle growth times (Wang et al. 2002).

In this paper, we first provide a description of the instrument and its calibration. Following this, the f-SMPS is applied to several sampling scenarios: (1) in a chamber system used for studying atmospheric reactions and secondary organic aerosol formation; (2) a chassis dynamometer used for emissions testing of light-duty gasoline vehicles; (3) a Mobile Emissions Laboratory (MEL) used for emissions testing of HDD vehicles while traveling on the road. The results obtained from these three sampling scenarios demonstrate the utility of this instrument and provide new insight into processes occurring in each system.

INSTRUMENT DESIGN

f-SMPS

A schematic of the f-SMPS is provided in Figure 1. Briefly, the SMPS consists of a TSI Model 3077 ^{85}Kr neutralizer, a rDMA (Zhang et al. 1995), and a mCPC (Wang et al. 2002). It is noted that the charge neutralizer will introduce a mixing time prior to analysis by the rDMA-mCPC that could effectively reduce the time resolution of the incoming particle stream. The use of a high throughput lower dead volume charge neutralizer will reduce these "mixing" effects. All required volumetric sample flows are actively controlled via a proportional-integral-differential (PID) control scheme with each flow rate measured as the pressure drop through a laminar flow element. The total system flow is 11 L min^{-1} with a 10:1 (particle-free):(polydisperse aerosol) split ratio. System control and data acquisition are provided by a software package written in LabView (National Instruments, Austin, TX). The entire system is designed and plumbed with minimal dead volume.

rDMA

The rDMA consists of two concentric, parallel disks separated by a gap of 10 mm. Aerosol flow tangentially enters the outer perimeter of one disk and is directed radially inward toward an exit at the center of the disk. Sheath flow enters the rDMA at the outer perimeter of the opposite disk. Excess flow exits through the center of the first disk. Charged particles are classified by electrical mobility diameter by migrating across the gap and out of the exit of the rDMA. Migration across the gap is achieved by exponentially ramping the voltage applied across the gap. Further descriptions of the rDMA are available in the literature (Zhang et al. 1995).

mCPC

The mCPC was selected to optimize the particle detection response time after exiting the rDMA. Thirty percent of the 1 lpm inlet flow to the mCPC is filtered by a HEPA and is saturated with n-butanol (BuOH) by flowing over a 65°C BuOH reservoir. The remainder of the flow enters the mCPC where it is turbulently mixed with the BuOH-laden air. The particles are grown to a detectable size as the mixed stream passes through a 10°C condenser. Particles are detected by a laser counter and acquired by a computer data acquisition system written in LabView. A further description of the mCPC is available in the literature (Wang et al. 2002).

Data Inversion

A matrix inversion routine developed by Collins et al. (2001) converts the count versus time signal into size distributions. The inversion program applies the theoretical rDMA transfer function, after accounting for instrument delay times, diffusional broadening, charging efficiency, and transmission efficiency of the aerosol through the instrument.

Instrument Calibration and Intercomparisons

Comparison to a Traditional SMPS

The f-SMPS was operated in series with a TSI Model 3081L cDMA to ascertain the effect of scan speed on the detected size

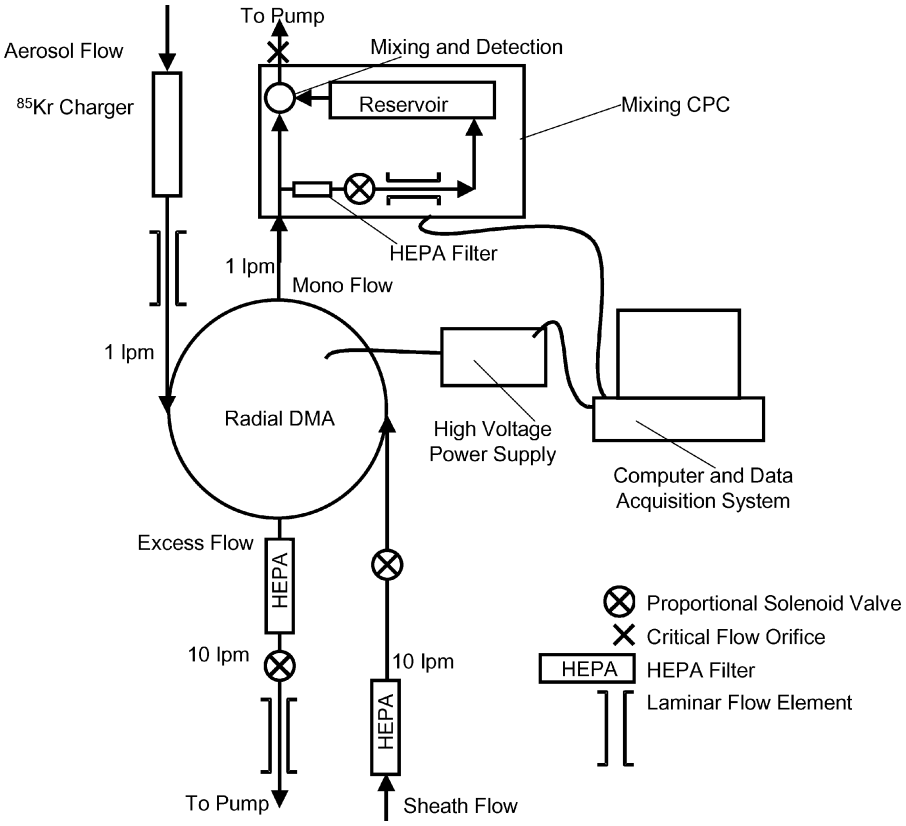

FIG. 1. Schematic of the f-SMPS.

distribution. The cDMA was equipped with a TSI Model 3077 ^{85}Kr neutralizer on its inlet and was operated at a fixed voltage to transmit dry, 65 nm $(NH_4)_2SO_4$ particles. The monodisperse aerosol exiting the cDMA was then delivered to the rDMA of the f-SMPS. Figure 2 shows the 65 nm preclassified particle size distribution as detected by the f-SMPS at scan speeds of 5, 10, 30, 45, and 60 seconds. The total number of particles detected (total area under the curve) was equivalent with only slight peak distortion seen at the highest scan speeds.

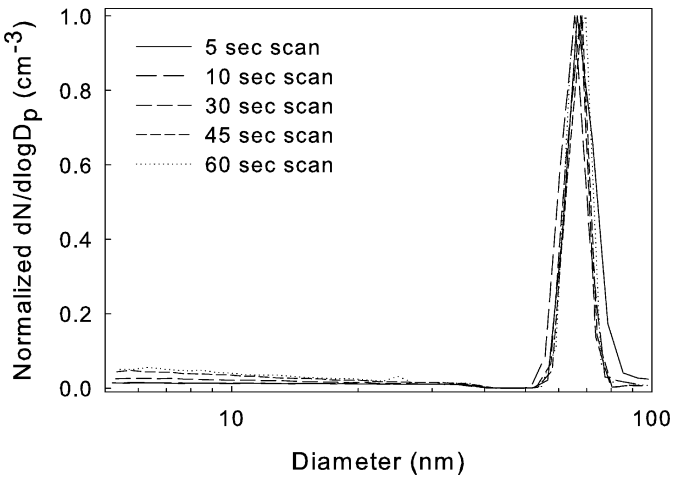

FIG. 2. Results of tandem DMA testing. cDMA was operated at a steady voltage to select 65 nm particles while the f-SMPS was operated at five different scan speeds.

The f-SMPS was also operated in parallel with a standard SMPS equipped with a TSI Model 3081L cDMA and a TSI Model 3760A CPC. In the configuration used at CE-CERT (10:1 sheath:aerosol flow; 2.75 LPM total flow), this instrument has the capability to detect particles in the range of 28–703 nm. An $(NH_4)_2SO_4$ aerosol was generated using a nebulizer (Liu and Lee 1975), dried and sent to the inlet of both instruments. Comparisons of size distributions were performed with the traditional SMPS operating at a scan speed of 300 seconds, while the f-SMPS was operated at 60, 10, 5, and 2.5 second scan speeds. Excellent agreement is seen for the size distributions (Figure 3) between the traditional SMPS (300-second scan speed) and the f-SMPS operating at speeds up to 2.5 seconds.

Time Constants

Improvements in SMPS scan speed require the minimization of the transport time between the DMA outlet and the CPC detector (plumbing time) and the mixing time constant within the CPC. The time constants for the mCPC were obtained by pulsing carbon particles generated by a 15 kV spark across two carbon electrodes separated by a distance of several millimeters

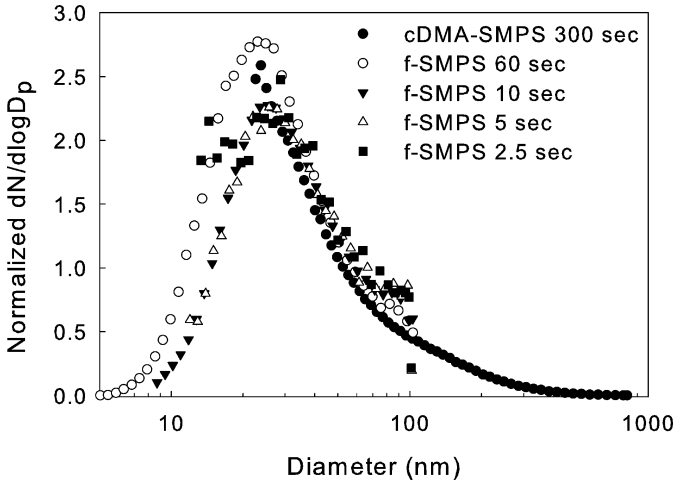

FIG. 3. Size distributions obtained using a traditional SMPS operated in parallel with a f-SMPS. The traditional SMPS was operated at a scan speed of 300 seconds while the f-SMPS was operated at scan speeds of 60, 10, 5, and 2.5 seconds. Size distributions were normalized by total number concentration in the 3–103 nm size range.

(Schwyn et al. 1988). The aerosol generator was connected to the inlet of the mCPC using Swagelok fittings to match the plumbing that would be present if the rDMA was connected. A mixing time (τ_{mix}) of 10.4 $\pm$ 1.2 ms was measured from the exponential decay of the response of the mCPC after aerosol generation ceased (see Figure 4). A plumbing time (τ_{plumb}) of 80 $\pm$ 4.1 ms was measured as the delay time between aerosol generation and detection by the mCPC.

Application to a Smog Chamber Studying SOA Formation

The f-SMPS was used to investigate the aerosol forming potential of whole reformulated gasoline in a smog chamber. The use of a smog chamber provided a well-controlled laboratory setting to initially examine the performance of the f-SMPS. Tests were conducted in an indoor 18 m^3 FEP Teflon reactor (Na et al.

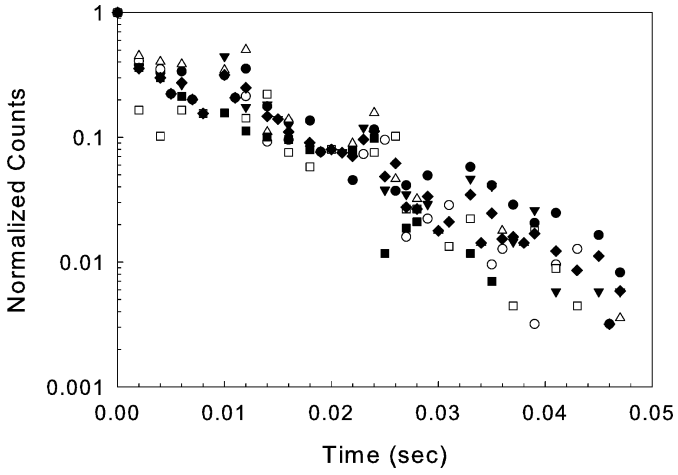

FIG. 4. Results of six measurements of the mCPC mixing time.

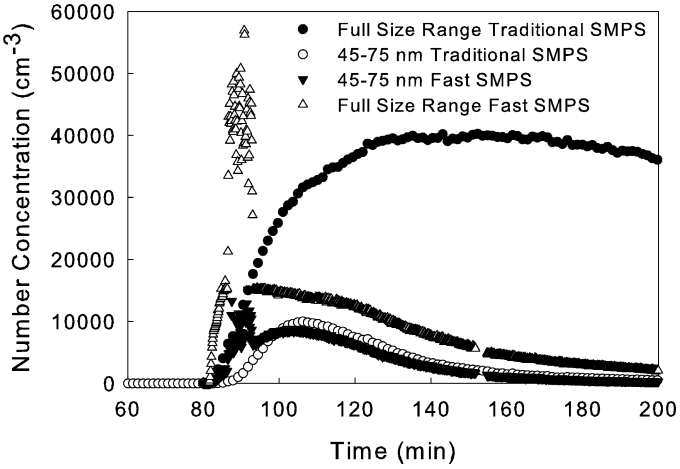

FIG. 5. Particle number concentration observed in smog chamber by a traditional and f-SMPS operated in parallel.

2004) with a 2.5 m^{-1} surface area to volume ratio. During these tests, whole gasoline was evaporated into the reactor and mixed with 400 ppb NO_x and 300 ppb propene followed by irradiation with 64 black lights. PM size distributions in the chamber were monitored by a traditional SMPS (cDMA operated at scan speeds of 300 seconds) as well as the f-SMPS (operated at scan speeds of 5 seconds). Total particle number concentration detected by each instrument is shown in Figure 5. The f-SMPS initially detects a higher total particle number concentration than the traditional SMPS, as these two instruments have different lower detection limits for particle size: 4 and 28 nm, respectively. As the reaction progresses, the peak of the particle size distribution quickly passes the maximum size of the f-SMPS (98 nm) with the result of the traditional SMPS measuring a larger total number concentration than the f-SMPS. The particle number concentration in the range of 45 to 75 nm is also presented in Figure 5. The smaller range of particle size provides a direct comparison of both instruments while minimizing potential size end effects for both instruments. Particle number concentration calculated for the range of overlap of the two instruments shows excellent agreement (within 10%) for the duration of the experiment. The difference between the f-SMPS and traditional SMPS is greater than 10% during the nucleation event (86–93 min).

The sudden rise and fluctuations of the number concentration seen by the fast-scan instrument correspond with multiple nucleation events occurring within the chamber. This indicates an inhomogeneity in the reactor not detected by the slower cDMA. It was confirmed that nucleation was not induced within the instrument by placing a HEPA filter at the inlet of the fast-scan instrument during a repeat experiment. With the HEPA filter in place, the fast-scan instrument did not detect any particles for the duration of the experiment. The particulates generated during the nucleation event are too small to be detected by the traditional SMPS.

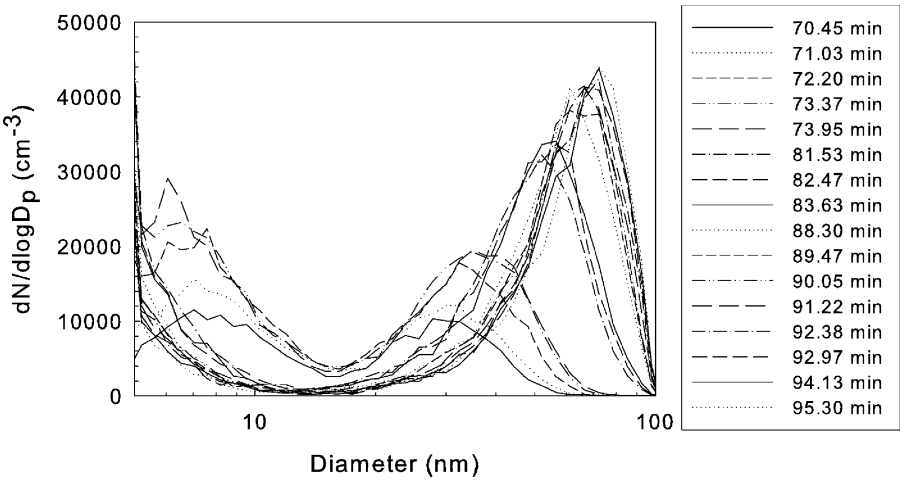

FIG. 6. Size distributions obtained at different times during smog chamber experiments. The solid vertical line represents the lower size limit of the cDMA.

Particle size distributions before and after the nucleation event can be seen in Figure 6. Although continuous data are available, only 1 distribution per minute (average of 10 scans) has been selected to show the growth of nuclei mode particles as the reaction progresses. Distributions from the multiple nucleation bursts are not shown here, as the time scale for nucleation events was faster than could be resolved with a 5 second scan speed. Early in the experiment, the presence of a large number of very small particles can clearly be seen by the f-SMPS. Shifts in both the nucleation and condensation peak sizes can be seen as smaller particles grow to larger sizes due to condensation and coagulation.

Sampling Combustion Generated Aerosols

Chassis Dynamometer Testing

Chassis dynamometer testing of a model year 2003 light-duty vehicle certified to Super Ultra-Low Emissions Vehicle (SULEV) standards were conducted in CE-CERT's Vehicle Emissions Research Laboratory (VERL). VERL consists of a Burke E. Porter single-roll (1.22 m OD) electric chassis dynamometer and a 0.254 m ID dilution tunnel. The vehicle exhaust was connected directly into the dilution tunnel via a thermally insulated coupling. Dilution air is preconditioned by a HEPA filter and charcoal filter to remove particulate matter and hydrocarbons. The vehicle was operated on the Federal Test Procedure (FTP) test cycle specified in the Code of Federal Regulations for the certification testing of light-duty vehicles. The cycle consists of three phases. The first phase (505 seconds in duration) is performed after the vehicle has been allowed to "soak" for 12 hours in ambient conditions. This results in a cold-start of the engine, followed by the prescribed driving cycle. The second phase (864 seconds in duration) is considered a hot phase, in which the vehicle is operated over a prescribed speed trace. Following the second phase, the vehicle is allowed to cool down for 10 minutes and a repeat of the first phase speed trace is performed for the third phase. Dilute exhaust (the total exhaust dilution ratio was 16.6, 26.7, and 19.9 for Phase 1, 2, and 3 of the FTP cycle, respectively) was sampled by the f-SMPS through ports in the dilution tunnel. Figure 7 shows the total number concentration of PM in the dilution tunnel as the vehicle is operated over the FTP cycle. The average tunnel background concentration is shown in Figure 7 as the dashed line. Aside from hard accelerations and cold-start emissions, the concentration in the dilution tunnel throughout the test was near the dilution tunnel background levels ($\sim$400 cm^{-3}). Similar to previous findings, the highest number concentrations of PM are encountered during the cold-start phase of the FTP (Maricq 1999). Cold-start emissions are influenced by both catalyst light-off time (fast) and the time for the engine/lubricating oil (slower) to reach optimal operating temperatures. In comparison to the first phase, the third phase (exactly the same speed trace with the vehicle warmed up) yields much lower PM concentrations. Peaks in number concentration seen during the hard accelerations of the first phase of the FTP were not seen during the third phase. The hard acceleration in the FTP (Phase 1: t = 166 s) shows the largest peak in particle number concentration. The size distributions during this event are show in Figure 8. The scan at t = 217 seconds was obtained during the hardest acceleration (greatest rate of acceleration). It can be seen from these distributions that during the hardest part of the acceleration (t = 217 seconds) a majority of the particles are above 15 nm. At t = 224 seconds, the peak of the acceleration (vehicle speed is at a maximum), there is a burst of PM below 10 nm.

On-Road Heavy-Duty Diesel (HDD) Vehicle Testing

Transient particle size distributions for a 2000 Caterpillar C-15 HDD engine installed in a Freightliner tractor operated on-road were obtained using CE-CERT's Mobile Emissions Laboratory (MEL). The MEL consists of a full-scale dilution

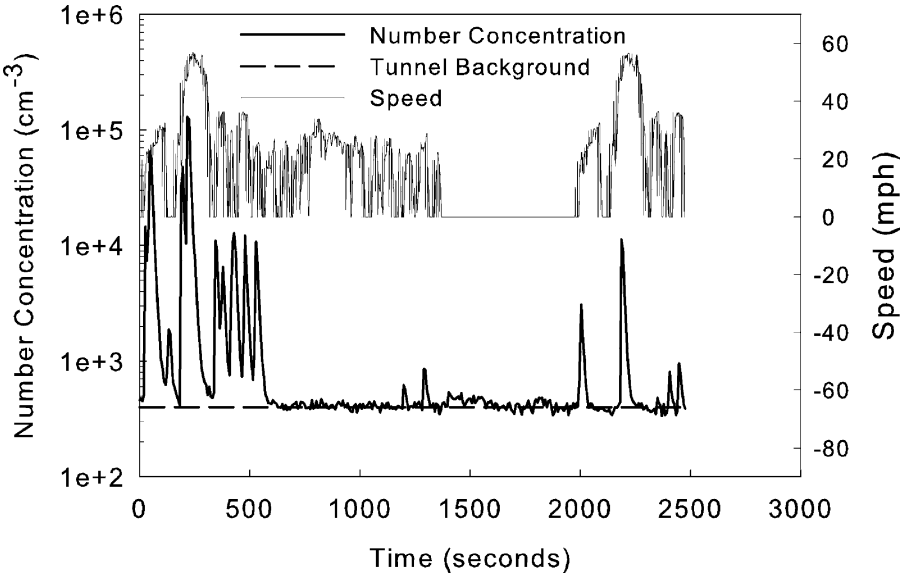

FIG. 7. PM number concentration during the FTP cycle. Solid vertical lines denote Phase 1, Phase 2, Hot Soak, and Phase 3, respectively.

tunnel housed inside a 53-foot trailer. Testing is conducted as the vehicle is driven over the road with total exhaust plumbed directly into the dilution tunnel through a flexible stainless steel snorkel. Inside the laboratory, PM samples are drawn through a secondary dilution system which provides additional dilution of the exhaust as well as strict control of the sample temperature at $47 \pm 5^{\circ}$C. Further descriptions of the MEL and secondary dilution system can be found in Cocker et al. (2004a, b). Testing was performed on an eastbound section of freeway 10 in Southern California. Rather than perform a driving cycle on the road, the driver was instructed to follow the flow of traffic. Several types of traffic and road conditions were encountered (cruising, uphill cruising, downhill cruising, accelerations, and travel through a weigh station). This enabled the collection of data for various operating modes of the engine. Figure 9 shows the particle number concentration (uncorrected for dilution) and speed trace for a portion of the test in which the truck encountered uphill, downhill, and low-speed driving. High particle concentrations were observed during accelerations and operation at high vehicle speeds on a grade. Truck operating data (collected from the engine's Electronic Control Module) show that these are instances of high engine load. A significant decrease ($\sim$50%) in number concentration can be seen as the road changes from an uphill grade to downhill driving.

As different driving modes were encountered during the on-road testing, individual size distributions during these events were grouped together and average size distributions were calculated. Size distributions for each grouping are found in

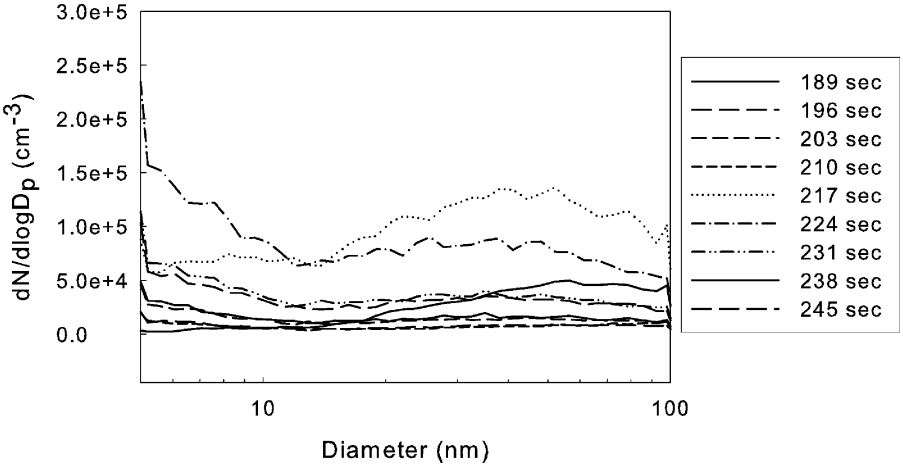

FIG. 8. PM size distributions from a SULEV vehicle observed during the hard acceleration of the FTP cycle.

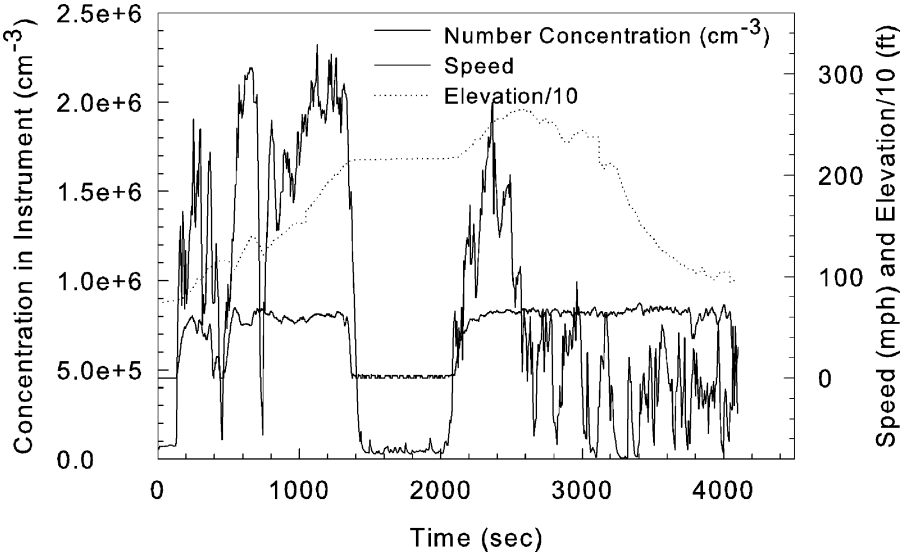

FIG. 9. Particle number concentration during on-road testing of a HDD vehicle. Concentration values are not corrected for the effects of dilution ratio.

Figure 10. Grouping was performed based on parameters described in Table 1. Peaks at ~85 nm (typically associated with combustion) were observed for all conditions. Similar to previous findings a peak was seen at 65 nm (Kweon et al. 2002) although in our work it was only observed for the accelerations and flat cruises. A peak at 15 nm can be seen for all driving modes except during uphill and downhill cruising.

The presence of a peak at 15 nm can be explained by the differences in driving conditions. During accelerations the engine operation is transient. During flat cruises and travel through the weigh station, the vehicle speed is constant, however, the engine is not maintained at a constant load. This transient engine operation is markedly different than the near steady-state operation encountered during uphill cruising. We have previously seen that organic carbon emissions are quite high during transient engine operation compared with near steady-state operation where elemental carbon emissions dominate (Shah et al. 2004). Several researchers have reported the organic fraction of diesel PM to consist primarily of lubricating oil (Zielinska 2003; Rogge et al. 1993). It is surmised that the peak observed at 15 nm during the transient operations is attributable to the nucleation of organic carbon (stemming from the emissions of lubricating oil) resulting from the transient engine operation. Sakurai et al. (2003), also found lubricating oil to contribute to nano-particle emissions diesel engines. Using a Thermal Desorption Particle Beam Mass Spectrometer and tandem DMAs, they investigated the chemical composition and volatility of diesel nano-particles. Results from their work demonstrated the significant contribution of lubricating oil to nano-particle production. Size selected particles with a diameter of 26 nm consisted of lubricating oil condensed on the surface of either nucleated sulfuric acid or nucleated lubricating oil.

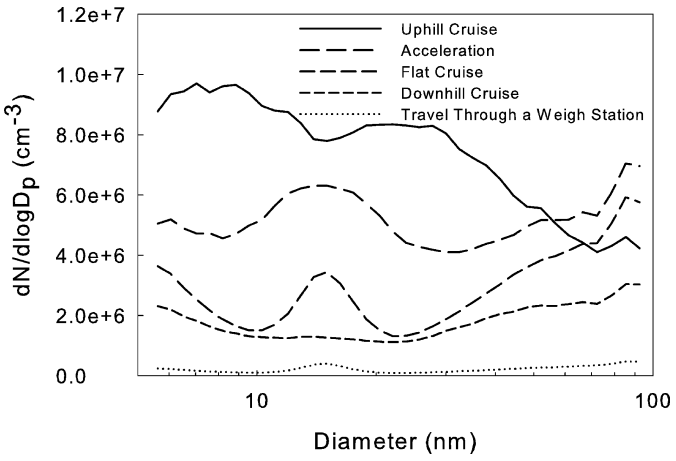

FIG. 10. On-road size distributions (corrected for dilution) observed during different vehicle operating modes of a HDD vehicle.

TABLE 1
Factors used to determine various vehicle operating modes

	Vehicle speed (mph)	Acceleration (ft sec^{-2})	Grade (ft mi^{-1})
Uphill cruising	50–60	N/A	>62 (1.2%)*
Downhill cruising	50–60	N/A	<−62 (−1.2%)*
Flat cruising	50–60	N/A	N/A
Accelerating	Increasing	<1.03	N/A

*Percent grade was calculated as change in elevation divided by distance traveled.

CONCLUSIONS

This work has demonstrated the utility of a f-SMPS in a variety of systems. The instrument has shown good comparison with traditional SMPS systems while achieving response times on time scales that allow for the examination of transient size distributions generated from combustion sources such as gasoline and diesel vehicles. For the smog chamber studies, the f-SMPS allowed for the examination of particle generation early in the reaction and indicated that multiple nucleation bursts were occurring within the chamber. Although the f-SMPS was not capable of elucidating the size distributions during this event, its scan speed can be further decreased to better capture these events. Results from chassis dynamometer testing of a SULEV vehicle have shown particle production is highest during the first phase and hard accelerations in the FTP. Particle number concentrations after vehicle warm-up are on the same order of magnitude as the dilution tunnel background. In its current configuration, the instrument has been optimized for installation into CE-CERT's MEL. Preliminary on-road testing of a heavy-duty diesel vehicle has shown the instrument to be robust and rugged enough to handle the rough ride encountered on the road. Emissions testing of the vehicle has shown marked differences in size distributions obtained during different HDD vehicle operating conditions.

ACKNOWLEDGMENTS

The authors would like to acknowledge Richard Flagan of Caltech, Jian Wang of Brookhaven National Laboratories, and Donald Collins of Texas A&M University for technical advice throughout the development of this instrument. We would also like to thank the staff and students at CE-CERT assistance in building and testing the instrument. This work was supported by the California Energy Commission and the California Air Resources Board.

REFERENCES

Allen, J. O., Mayo, P. R., Hughes, L. S., Salmon, L. G., and Cass, G. R. (2001). Emissions of Size Segregated Aerosols from On-Road Vehicles in the Caldecott Tunnel, *Environ. Sci. Technol.* 35:4189–4197.

Caldow, R. (2004). An Engine Exhaust Particle Sizer Spectrometer for Transient Emission Particle Measurements, *Proceedings of the 14th CRC On-Road Vehicle Emissions Workshop*. San Diego, CA.

Cocker, D. R., Shah, S. D., Johnson, K., Miller, J. W., and Norbeck, J. M. (2004). Development and Application of a Mobile Laboratory for Measuring Emissions from Diesel Engines. 1. Regulated Gaseous Emissions, *Environ. Sc. Technol.* 38:2182–2189.

Cocker, D. R., Shah, S. D., Johnson, K. C., Miller, J. W., and Norbeck, J. M. (2005). Development and Application of a Mobile Laboratory for Measuring Emissions From Diesel Engines. 2. Sampling for Toxics and Particulate Matter, *Environ. Sci. Technol.* 38(24):6809–6816.

Collins, D. R., Cocker, D. R., Flagan, R. C., and Seinfeld, J. H. (2004). The Scanning DMA Transfer Function, *Aerosol Sci. Technol.* 38:833–850.

Collins, D. R., Flagan, R. C., and Seinfeld, J. H. (2002). Improved Inversion of Scanning DMA Data, *Aerosol Sci. Technol.* 36:1–9.

Flagan, R. C. (1998). History of Electrical Aerosol Measurements, *Aerosol Sci. Technol.* 28:301–380.

Han, H. S., Chen, D. R., Pui, D. Y. H., and Anderson, B. E. (2000). A Nanometer Aerosol Size Analyzer (ASA) for Rapid Measurement of High-Concentration Size Distributions, *J. Nanoparticle Research* 2:43–52.

Keskinen, J., Pietarinen, K., and Lehtimaki, M. (1992). Electrical Low Pressure Impactor, *J. Aerosol Sci.* 23:353–360.

Khlystov, A., Kos, G. P. A., ten Brink, H. M., Mirme, A., Tuch, T., Roth, C., and Kreyling, W. G. (2001). Comparability of Three Spectrometers for Monitoring Urban Aerosol, *Atmos. Environ.* 35:2045–2051.

Kittelson, D. B., Watts, W., and Johnson, J. (2001). Particle Measurement Methodology: On-Road and Laboratory Measurements of Nanoparticles from Diesel Engines, *Proceedings of the 11th CRC On-Road Vehicle Emissions Workshop*, San Diego, CA.

Kittelson, D. (2002). Instruments for Measurement of Size and other Metrics of Exhaust Particles, *Workshop on Vehicle Exhaust Particulate Emission Measurement Methodology.* San Diego, CA.

Kweon, C. B., Foster, D. E., Schauer, J. J., and Okada, S. (2002). Detailed Chemical Composition and Particle Size Assessment of Diesel Engine Exhaust, *SAE Technical Paper Series 2002-01-2670.*

Liu, B. Y. H., and Lee, K. W. (1975). An Aerosol Generator of High Stability, *A.I.H.J.* 36:861–865.

Maricq, M. M., Podsiadlik, D.H., and Chase, R.E. (1999). Gasoline Vehicle Particle Size Distributions: Comparison of Steady State, FTP, and US06 Measurements, *Environ. Sci. Technol.* 33:2007–2015.

Maricq, M. M., Podsiadlik, D. H., and Chase, R. E. (2000). Size Distributions of Motor Vehicle Exhaust PM: A Comparison Between ELPI and SMPS Measurements, *Aerosol Sci. Technol.* 33:239–260.

Moisio, M., and Niemela, V. (2002). Device for Continuous Measurement of Density and Mass Concentration of Vehicle Exhaust Aerosol, *IAC.*

Na, K., Song, C., and Cocker, D. R. (2004). Formation of Secondary Organic Aerosol from the Reaction of Styrene with Ozone in the Presence and Absence of Ammonia and Water, *Environ. Sci. Technol.* Submitted 2005.

Rogge, W. F., Hildemann, L. M., Mazurek, M. A., Cass, G. R., and Simoneit, B. R. T. (1993). Sources of Fine Organic Aerosol. 2. Noncatalyst and Catalyst Equipped Automobiles and Heavy-Duty Trucks, *Environ. Sci. Technol.* 27:636–651.

Sakurai, H., Tobias, H. J., Park, K., Zarling, D., Docherty, K. S., Kittelson, D. B., McMurry, P. H., and Ziemann, P. J. (2003). On-Line Measurements of Diesel Nanoparticle Composition and Volatility, *Atmos. Environ.* 37:1199–1210.

Schwyn, S., Garwin, E., and Schmidt-Ott, A. (1988). Aerosol Generation by Spark Discharge, *J. Aerosol Sci.* 19:639–642.

Shah, S. D., Cocker, D. R., Miller, J. W., and Norbeck, J. M. (2004). Emission Rates of Particulate Matter and Elemental and Organic Carbon from In-Use Diesel Engines, *Environ. Sci. Technol.* 38:2544–2550.

Shi, J. P., Harrison, R. M., and Brear, F. (1999). Particle Size Distribution from a Modern Heavy Duty Diesel Engine. *Science of the Total Environment* 235:305–317.

Tammet, H., Mirme, A., and Tamm, E. (1998). Electrical Aerosol Spectrometer of Tartu University, *J. Aerosol Sci.* 29:S427–S428.

Wang, J., McNeill, V. F., Collins, D. R., and Flagan, R. C. (2002). Fast Mixing Condensation Nucleus Counter: Application to Rapid Scanning Differential Mobility Analyzer Measurements, *Aerosol Sci. Technol.* 36:678–689.

Zielinska, B. (2003). The Correlation of Lubricating Oil and Fuel Organic Composition with Tailpipe Emissions, *Proceedings of the 13th CRC On-Road Vehicle Emissions Workshop*, San Diego, CA.

Zhang, S. H., Akutsu, Y., Russell, L., Flagan, R., and Seinfeld, J. (1995). Radial Differential Mobility Analyzer, *Aerosol Sci. Technol.* 23:357–372.